YTHDF1 regulates immune cell infiltration in gastric cancer via interaction with p53

QUAN LIAO[1,2] and JIANPING XIONG[1,2]

[1]Department of Oncology, The First Affiliated Hospital of Nanchang University;
[2]Jiangxi Key Laboratory for Individualized Cancer Therapy, Nanchang, Jiangxi 330006, P.R. China

Abstract. The N^6-methyladenosine reader YTH N^6-methyladenosine RNA binding protein 1 (YTHDF1) has been assessed in several tumor types and holds significance in the tumor microenvironment (TME). Furthermore, p53, an important tumor suppressor, is closely associated with the TME. The present study evaluated the roles of YTHDF1 and p53 in regulating the TME in gastric cancer (GC). Genetic alterations in the YTH domain family were analyzed using the cBioPortal database. Expression of YTHDF1 in GC cells and tissues was assessed using the Tumor Immune Estimation Resource (TIMER), Gene Expression Profiling Interactive Analysis (GEPIA), University of Alabama at Birmingham Cancer data analysis portal and Tumor-Immune System Interactions and Drug Bank (TISIDB) databases, along with reverse-transcription-quantitative PCR and western blotting in GC. The prognostic value of multiple tumors was determined using Kaplan-Meier analysis. Correlation analyses were performed using the TIMER, TISIDB and GEPIA databases. Protein-protein interactions of YTHDF1 were predicted using GeneMANIA and HitPredict, and confirmed using co-immunoprecipitation. Gene Ontology and Kyoto Encyclopedia of Genes and Genomes enrichment analyses of the YTHDF1 functional network in GC were performed using LinkedOmics. Genetic alterations revealed that, among the YTH domain family members, YTHDF1 had the highest alteration in GC and was associated with a shorter survival. Additionally, YTHDF1 was significantly negatively associated with the level of CD8+ T cells, B cells, macrophages, dendritic cells (DCs) and neutrophils in GC. Furthermore, tumor associate macrophage-related and DC markers were significantly negatively correlated with YTHDF1 expression, whilst regulatory T cells and T cell exhaustion markers were significantly negatively associated with YTHDF1 expression. In addition, compared with that in p53-nonmutant GC cells, YTHDF1 expression was significantly higher in p53-mutated GC cells, indicating a potential association between YTHDF1 and p53. Analyses using the GeneMANIA and HitPredict databases, and co-immunoprecipitation, demonstrated that YTHDF1 interacted with p53. In conclusion, the findings of the present study indicate that YTHDF1 is associated with a poor prognosis and serves an important role in the TME of GC. We hypothesize, for the first time to the best of our knowledge, that YTHDF1 regulates immune cell infiltration by interacting with p53 in GC, which provides a promising direction for future research.

Introduction

Gastric cancer (GC), which ranks fifth in incidence and fourth in mortality among all types of cancer in the world, continues to pose a significant health challenge worldwide. Despite notable advancements in surgery, chemotherapy and radiation therapy, the mortality rate of GC remains high (1), with >1 million new cases and 769,000 deaths reported worldwide in 2020 (2). Immunotherapy has revolutionized the treatment of many types of human cancers and has been the cornerstone of success in the treatment of several cancers (3). Although certain patients with GC achieve dramatic and durable responses to immunotherapy with a superior safety profile, only a few patients benefit from this treatment. The tumor microenvironment, especially immune cell infiltration, serves an important role in the immunotherapy response. Considering the promise of immunotherapy, further research on the tumor microenvironment (TME) is necessary.

N^6-methyladenosine (m6A), the most prevalent internal modification of eukaryotes, was discovered in the 1970s (4). The formation of m6A is a dynamic and reversible process. In general, a methyl group is installed on the N^6 position by 'writers' [methyltransferase-like (METTL)3, METTL14 and Wilms tumor 1-associated protein] and removed by 'erasers' [fat mass and obesity-associated protein (FTO) and AlkB homolog 5 (ALKBH5)] (5). These molecules regulate many biological functions. For example, METTL3/14 regulates the response of colorectal carcinoma and melanoma to anti-programmed cell death protein 1 (PD-1) therapy via interferon-γ-signal transducer and activator of transcription 1-interferon regulatory

Correspondence to: Professor Jianping Xiong, Department of Oncology, The First Affiliated Hospital of Nanchang University, 17 Yongwai Road, Donghu, Nanchang, Jiangxi 330006, P.R. China
E-mail: jpxiong0630@outlook.com

factor 1 signaling (6). FTO inhibits the stemness of ovarian cancer cells by enhancing cAMP signaling (7). ALKBH5 inhibits pancreatic cancer tumor development and chemosensitization by regulating Wnt signaling (8). The YTH domain family, serving as 'readers' of m6A, contains five members [YTH Domain Containing (YTHDC)1, YTHDC2, YTH m6A RNA binding protein (YTHDF)1, YTHDF2 and YTHDF3], each of which mediate different functions of m6A-methylated RNAs by recognizing m6A modification. YTHDC1 serves a pivotal role in RNA splicing and nuclear protein export (9). YTHDC2, which contains a helicase domain, maintains a gene expression program that facilitates meiotic progression by regulating the levels of m6A-modified germline transcripts (10). YTHDF2 promotes hepatocellular carcinoma stem cell phenotype and metastasis by regulating octamer-binding transcription factor 4 mRNA methylation, which is associated with a poor prognosis (11). YTHDF3 serves a critical role in breast cancer brain metastasis by enhancing the translation of ST6 N-acetylgalactosaminide α-2,6-sialyltransferase 5 and gap junction protein α1 (12).

YTHDF1 serves a pivotal role in regulating tumor proliferation and apoptosis (13), tumorigenesis and metastasis (14), and cell cycle progression and metabolism (15). In recent years, emerging evidence has indicated that YTHDF1 serves an important role in the tumor immune microenvironment (TIME). In breast cancer, YTHDF1 is closely associated with CD4 T cells, natural killer (NK) cells, monocytes and macrophages (16). Another study indicated that immune cell infiltration levels and immune markers in ovarian carcinoma are closely linked to YTHDF1 expression (17). Previous studies have suggested that YTHDF1 inhibits the tumor-suppressive effect of p53 and promotes tumor progression (18). However, whilst studies have hinted at the involvement of YTHDF1 in several cancers, a comprehensive understanding of its role in gastric cancer, particularly in association with p53, remains elusive. Therefore, the present study aimed to assess the roles of YTHDF1 and p53 in regulating the immune microenvironment of GC. Through an evaluation of YTHDF1 expression, its association with immune cell infiltration in GC, and its association with p53 mutations, we hypothesize, for the first time to the best of our knowledge, that YTHDF1 serves a crucial role in regulating immune cell infiltration by interacting with p53 in GC. This novel perspective provides a promising direction for future research.

Materials and methods

cBioportal database. The cBio Cancer Genomics Portal (https://www.cbioportal.org/) (19), which offers a visualization tool for the study and analysis of tumor gene data, provides a comprehensive approach to understanding genetics, epigenetics, gene expression and proteomics-based on molecular data derived from tumor tissues and cytology studies. In the present study, the cBioPortal database was used to analyze genetic alterations in the YTH family in GC. In brief, the following origin studies were selected: Gastric cancer (OncoSG, 2018) (20), stomach adenocarcinoma (Pfizer and UHK, Nature Genetics 2014) (21), stomach adenocarcinoma (TCGA, Firehose Legacy) (22), stomach adenocarcinoma (University of Tokyo, Nature Genetics 2014) (23) and stomach

adenocarcinoma (UHK, Nature Genetics 2011) (24). Subsequently, a query was performed using a gene list comprising YTHDF1, YTHDF2, YTHDF3, YTHDC1 and YTHDC2.

Tumor Immune Estimation Resource (TIMER) database analysis. The TIMER database (https://cistrome.shinyapps.io/timer/) (25), which detects the infiltration of immune cells into tumor tissues, provides six types of immune cell infiltration levels. Immune cells include B cells, CD4+ T cells, CD8+ T cells, neutrophils, macrophages and dendritic cells (DCs). This database consists of seven modules. In the present study, the association between YTHDF1 and immune cell infiltration was determined using a gene module. The specific settings were as follows: Gene symbol, YTHDF1; cancer types, stomach adenocarcinoma (STAD); and immune infiltrates, B cell, CD8+ T cell, CD4+ T cell, macrophages, neutrophils and DCs. Additionally, the 'SCNA' module was used to assess immune infiltration levels in GC with varying YTHDF1 copy number alterations. The parameters for this analysis were as follows: Gene symbol, YTHDF1; cancer types, STAD; and immune infiltrates, B cell, CD8+ T cell, CD4+ T cell, macrophages, neutrophils and DCs. Furthermore, a correlation module was used to analyze the relationship between YTHDF1 and several immune markers in GC. The following parameters were set: Cancer types, STAD; gene symbol (y-axis), YTHDF1; and gene symbol (x-axis), immune markers.

University of Alabama at Birmingham Cancer data analysis portal (UALCAN) database. The UALCAN data analysis portal (http://ualcan.path.uab.edu/) (26) is a comprehensive online resource that can be used to assess tumor subgroup gene expression based on different features. In the present study, the UALCAN database was used to analyze the association between YTHDF1 and tumor grade, p53 mutation status and microsatellite instability status in GC. In brief, the YTHDF1 expression level in stomach adenocarcinoma was evaluated by inputting the gene symbol. Subsequently, the expression level was analyzed in relation to tumor grade, p53 mutation status and microsatellite instability status using Clinical Proteomic Tumor Analysis Consortium (https://ualcan.path.uab.edu/cgi-bin/CPTAC).

Tumor-Immune System Interactions and Drug Bank (TISIDB) database. The TISIDB database (http://cis.hku.hk/TISIDB/) (27) is a powerful online resource with extensive data on tumor immunity. The database contains information on 988 genes associated with antitumor immunity and can precompute the associations between genes and the immune function of 28 tumor-infiltrating lymphocytes (TILs) for 30 cancer types from The Cancer Genome Atlas (TCGA). Additionally, the database includes genomic, transcriptomic and clinical data of 30 TCGA tumors. The analysis in the present study involved assessing associations between YTHDF1 expression, gastric tumor grade and molecular subtype. In brief, YTHDF1 was searched for in the 'Gene Symbol' dialog box. Following that, the Lymphocyte module was used to calculate Spearman's correlation coefficient for YTHDF1 expression and TILs across several human cancers. Subsequently, the lymphocyte types for the x-axis and cancer

types for the y-axis were selected to generate a plot for each lymphocyte type in a single cancer. Additionally, the association between YTHDF1 expression and the molecular subtypes of gastric cancer were analyzed using the subtype module.

Kaplan-Meier plotter analysis. The association between YTHDF1 and survival in multiple cancer types was analyzed using the Kaplan-Meier plotter (https://kmplot. com/analysis/) (28), which evaluates the correlation between 70,632 genes and prognosis across 21 human cancers. Using this database, a pan-cancer RNA-sequencing search was performed using YTHDF1 (221741_s_at, and an auto selected best cutoff) and overall survival (OS) to assess the relationship between YTHDF1 expression and OS in multiple human cancer types. Hazard ratios with 95% confidence intervals (CIs) and log-rank P-values were calculated to quantify the significance of this association.

Gene expression profiling interactive analysis (GEPIA) database. The GEPIA database (http://gepia.cancer-pku.cn/) (29) seamlessly integrates gene expression profiling data from the TCGA and Genotype-Tissue Expression (GTEx) projects to provide multiple data analyses and visualization capabilities. The correlation module was used to assess the relationships between genes related to T-cell exhaustion, namely PD-1, T-lymphocyte-associated protein 4, T cell immunoglobulin and mucin-domain-containing-3 (TIM-3), and the expression of YTHDF1. Associations between the expression of YTHDF1 and gastric cancer-related genes, such as KRAS, human epidermal growth factor receptor-2 (HER-2) and TP53, were also analyzed using this module. Regarding the specific settings, YTHDF1 was designated as Gene A for the x-axis, whilst individual genes associated with T-cell exhaustion or gastric cancer served as Gene B for the y-axis. Spearman's rank correlation coefficient was calculated. Subsequently, the STAD tumor was selected from 'TCGA Tumor' dialog box, STAD normal from the 'TCGA Normal' dialog box and stomach from the 'GTEx' dialog box. These selections were used to compile the dataset list, upon which the correlation analysis was performed.

GeneMANIA database. The GeneMANIA database (http://genemania.org/) (30), designed to predict the function of genes of interest, indexes 2,830 association networks containing 660,554,667 interactions mapped to 166,691 genes from nine organisms. This database enables users to predict gene-gene functional interaction networks from a provided gene list. In the present study, the GeneMANIA database was used to predict the interactions between YTHDF1 and the p53 pathway by searching for a gene list that included YTHDF1, p53, p21 and mouse double minute 2 (MDM2).

HitPredict database. HitPredict (http://www.hitpredict. org/) (31) integrates protein-protein interactions derived from high-throughput or small-scale trials in the IntAct, BioGRID, HPRD, MINT and DIP databases. In the present study, an interaction was identified between YTHDF1 and p53 by querying the HitPredict database with gene symbol YTHDF1 in *Homo sapiens* and evaluating the interaction between YTHDF1 and p53 using reliability scores as a metric.

LinkedOmics database. The LinkedOmics database (http://www.linkedomics.org/) (32) includes multiomics and clinical data for 32 types of cancer and 11,158 patients from TCGA. Initially, an analysis to identify genes that correlate with YTHDF1 expression in gastric cancer (GC) was performed through the following process: The STAD cohort, the HiSeq RNA dataset, YTHDF1 as the dataset attribute, HiSeq RNA as the target dataset, and the Pearson correlation test as the statistical method, were selected. Subsequently, the correlated genes were selected to perform Gene Ontology and Kyoto Encyclopedia of Genes and Genomes (KEGG) enrichment analyses using the Gene Set Enrichment Analysis tool.

Cell lines and cell culture. The GC cell lines, namely HGC-27, AGS and MKN-45, the human normal gastric mucosa epithelial cell line GES-1, and the 293T cell line, were purchased from the Cell Bank of Type Tissue Culture Collection of The Chinese Academy of Sciences (Shanghai, China). All cells were cultured in DMEM (Hyclone; Cytiva) with 10% FBS (Gibco; Thermo Fisher Scientific, Inc.) and 1% penicillin/streptomycin in an incubator with 5% CO_2 at 37˚C for 24-48 h. All cells were confirmed to be mycoplasma-free and authenticated using PCR analysis.

Plasmid and transfection. Human YTHDF1 was subcloned into Myc-His-pcDNA3.1. The full-length cDNA of YTHDF1 was amplified using PCR, with primers that were designed using the National Center for Biotechnology Information Primer-BLAST tool (33). Prior to synthesis, protective bases (CCG) and specific enzyme cleavage sites (Xho I: 5'-CTCGAG-3' for the forward primer and EcoR I: 5'-GAATTC-3' for the reverse primer) were appended to the 5' ends of the primers. The sequences of these primers were as follows: Forward, 5'-CCGCTCGAGATGTCGGCCACCAGC GTGGA-3' and reverse, 5'-CCGGAATTCTCATTGTTTGTT TCGACTCTGC-3'. The PCR assay was executed utilizing Taq Plus DNA Polymerase (cat. no. P101-01; Vazyme Biotech Co., Ltd.) in accordance with the following thermocycling conditions: Pre-denaturation at 95˚C for 8 min, followed by 38 cycles of denaturation at 94˚C for 30 sec, annealing at 55˚C for 30 sec and extension at 72˚C for 2 min. Subsequently, a final extension step was performed at 72˚C for 7 min. The resulting products were separated on a 2% agarose gel and visualized using UV imager (Tanon Science and Technology Co., Ltd.). After PCR amplification, both the amplified fragment and the empty vector (Myc-His-pcDNA3.1) underwent enzymatic cleavage. The reaction mixture (20 μl) consisted of 2 μl New England BioLabs buffer 2.1 (New England BioLabs, Inc.), 1 μl Xho I (New England BioLabs, Inc.), 1 μl EcoR I (New England BioLabs, Inc.), 2 μg of the fragment or 1 μg of the empty vector, and an appropriate amount of double-distilled water (ddH2O). The mixtures were incubated for 2 h at 37˚C. Subsequently, the cleaved fragment and empty vector were ligated using T4 ligase. The ligation reaction mixture (10 μl) contained 1 μl T4 ligase buffer (New England BioLabs, Inc.), 1 μl T4 ligase (New England BioLabs, Inc.), 20 ng of the empty vector, 120 ng of the fragment, and an appropriate amount of ddH2O. The ligation mixtures were incubated for 16 h at 16˚C. Myc-His-pcDNA3.1 was used as a negative control in the YTHDF1 overexpression experiment. The plasmid encoding

p53 (pcDNA3.1-p53) was donated by Professor Xiang Zhou (Fudan University Shanghai Cancer Center) and plasmids expressing the empty vector (pcDNA3.1) were used as a negative control. Plasmids (10 μg Myc-His-pcDNA3.1-YTHDF1, pcDNA3.1-p53 or corresponding empty vector) were transiently transfected (at 37°C) into 293T cells that had been seeded overnight on 10 cm dishes using polyethylenimine (Sigma-Aldrich; Merck KGaA). The cells were harvested 48 h post-transfection for subsequent experiments.

Clinical specimens. GC and adjacent normal tissue specimens were collected after surgery at the First Affiliated Hospital of Nanchang University (Nanchang, China) and were promptly frozen in liquid nitrogen and stored in -80°C until use. All patients provided signed informed consent before sample collection. The present study was approved by the Ethics Committee of First Affiliated Hospital of Nanchang University.

Reverse transcription(RT)-quantitative (q)PCR. TRIzol™ reagent (Takara Biotechnology Co., Ltd.) was used to extract total RNA from the GC cell lines. The PrimeScript™ RT reagent kit (cat. no. RR047A; Takara Biotechnology Co., Ltd.) and TB Green™ premix Ex Taq (cat. no. RR820B Takara Biotechnology Co., Ltd.) were used to detect the mRNA levels of YTHDF1 according to the manufacturer's instructions. The fluorophore used in present study was carboxyfluorescein (MilliporeSigma). The qPCR assay employed the following thermocycling conditions: An initial pre-denaturation step at 95°C for 30 sec, followed by 40 cycles of denaturation at 95°C for 30 sec, annealing at 60°C for 30 sec and extension at 95°C for 15 sec. Subsequently, a final extension step was performed at 60°C for 60 sec and 95°C for 15 sec. The relative expression of YTHDF1 mRNA in GC cell lines was calculated using the $2^{-\Delta\Delta Cq}$ method (34) and normalized to GAPDH. The primers used were as follows: YTHDF1 (forward) 5'-ACC TGTCCAGCTATTACCCG-3' and (reverse) 5'-TGGTGAGGT ATGGAATCGGAG-3'; GAPDH (forward) 5'-CGCTCTCTG CTCCTCCTGTTC-3' and (reverse) 5'-ATCCGTTGACTC CGACCTTCAC-3'.

Immunoblotting. Proteins from GC tissues or cells were obtained using RIPA buffer (containing 1% protease/phosphatase inhibitor; Applygen Technologies, Inc.). The protein concentration was measured utilizing the BCA protein assay kit (cat. no. P0010; Beyotime Institute of Biotechnology). The proteins (20 μg) were separated by 10% SDS-PAGE and electroblotted onto polyvinylidene difluoride membranes (Bio-Rad Laboratories, Inc.). The membranes were blocked with 5% milk for 1 h at room temperature and then incubated with primary antibodies against YTHDF1 (1:1,000; cat. no. 17479-1-AP; Proteintech Group, Inc.) and GAPDH (1:5,000; cat. no. 60004-1-Ig; Proteintech Group, Inc.) overnight at 4°C. Following a wash with TBST (containing 0.1% Tween), the membranes were incubated for 1 h at room temperature with the appropriate secondary antibodies conjugated to horseradish peroxidase (HRP-conjugated affinipure goat anti-rabbit IgG; 1:10,000; cat. no. SA00001-2; or anti-mouse IgG; 1:10,000; cat. no. SA00001-1; Proteintech Group, Inc.). GAPDH was used as an internal control. Proteins were visualized with the ECL chemiluminescence reagent (Shanghai Yeasen Biotechnology, Co., Ltd.).

Immunohistochemistry (IHC) of YTHDF1 and its association with lymphocyte subsets. To assess the relationship between YTHDF1 expression and lymphocyte subsets in clinical samples, the expression of YTHDF1 was first assessed in GC tissues using IHC. In brief, paraffin-embedded sections of GC tissue (5-μm thick sections, fixed with 4% paraformaldehyde at room temperature for 20 min) were deparaffinized and rehydrated using different concentrations of ethanol (anhydrous ethanol for 5 min, 95% ethanol for 5 min, 90% ethanol for 5 min, 80% ethanol for 3 min and 70% ethanol for 3 min) at room temperature. Subsequently, the sections were incubated in a 3% H_2O_2 solution for 10 min at room temperature to eliminate endogenous peroxidase. Antigen retrieval was performed by heating the sections in citrate buffer at 95°C for 1 h. Then sections were blocked with 2% BSA (Origene Technologies, Inc.) for 20 min at room temperature. Subsequently, the sections were incubated with rabbit anti-human polyclonal YTHDF1 antibodies (1:100; cat. no. 17479-1-AP; Proteintech Group, Inc.) in a humidified box overnight at 4°C. Sections were then washed thrice with PBS, followed by incubation with a horseradish peroxidase system (cat. no. Ab6721; Abcam) and liquid DAB (cat. no. K346889-2; Dako; Agilent Technologies, Inc.) at room temperature. Finally, the sections were incubated in PBS containing diaminobenzidine for 10 min at room temperature. A light microscope (Ti-S-Fi1C; Nikon Corporation) was used for imaging at x100 magnification. The evaluation criteria were as follows: Staining intensity for YTHDF1 was scored as 0 (negative), 1 (weak), 2 (moderate) and 3 (strong). Staining extent was scored as 0 (0), 1 (1-25%), 2 (26-50%), 3 (51-75%) and 4 (76-100%). The product of the stain intensity and extent scores was regarded as the score index (SI). According to the SI scores, samples with SI score ≥6 were considered to have high YTHDF1 expression, whilst the rest were considered to have low YTHDF1 expression. Subsequently, data on lymphocyte subsets, analyzed by the laboratory department of the First Affiliated Hospital of Nanchang University using flow cytometry, were collected from the clinical medical records of each patient. Data were analyzed using GraphPad Prism 8.0.2 (Dotmatics). Unpaired Student's t-tests were used to assess the differences between the high and low YTHDF1 expression groups concerning total lymphocytes, total T, CD4+ T, CD8+ T, NK and B cells.

Immunoprecipitation. 293T cells were transfected with Myc-YTHDF1, p53 or control for 48 h at 37°C and treated with 20 μM MG132 (MedChemExpress) for 6 h before being harvested on the ice. Following that, proteins were extracted using lysis buffer [10 mM Tris, 150 mM NaCl, 1 mM Na2EDTA.2H2O, 3.5 mM SDS, 1 mM DTT and 1% NP-40 (pH 7.4)], and immunoprecipitation was performed using the anti-Myc or anti-p53 antibodies. In brief, 10 μg whole cell lysate were used as the input. A total of 500 μg protein was incubated with 2 μg anti-IgG (cat. no. 30000-0-AP; Proteintech Group, Inc.), 2 μg anti-p53 (cat. no. sc-126; Santa Cruz Biotechnology, Inc.) or 2 μg anti-Myc (cat. no. 10828-1-AP; Proteintech Group, Inc.) antibodies at 4°C for 4 h. Protein G beads (40 μl) (Santa Cruz Biotechnology, Inc.) were then added to the mixture, followed by incubation at 4°C for an additional 2 h. The beads were washed five times with 1 ml lysis buffer, with each wash involving centrifugation at 800 x g for 1 min at 4°C. Protein

complexes were detected by immunoblotting, as in the aforementioned description.

Statistical analysis. Most statistical analyses were automatically performed using online databases, following the statistical methods outlined in their respective databases. Additionally, the statistical analysis of experimental data was performed using GraphPad Prism 8.0.2 (Dotmatics). Specifically, for comparing data between two groups, an unpaired Student's t-test was used, whereas one-way ANOVA followed by Tukey's post hoc test was used for comparing ≥3 groups. P<0.05 was used to indicate a statically significance difference.

Results

YTHDF1 expression and prognostic value in GC. The cBio-Portal database was first used to determine genetic alterations in the YTH domain family among patients with GC. It was demonstrated that YTHDF1 had the highest alteration rate, observed in 10% of the cases, followed by YTHDF3, YTHDC2 and YTHDC1, with alteration rates of 5.0, 3.0 and 2.4%, respectively. The lowest alteration rate was for YTHDF2, at 2.3% (Fig. 1A).

Subsequently, the expression of YTHDF1 was assessed using the GEPIA and UALCAN databases. The results revealed a significant upregulation of YTHDF1 in GC samples compared with that in normal tissues (Fig. 1B and C). YTHDF1 expression was significantly associated with GC tumor grade, demonstrating a significant increase in poorly differentiated GC (Fig. 1D). Similar results were observed in the TISIDB database analysis (Fig. 1E). Furthermore, YTHDF1 overexpression was significantly associated with microsatellite instability-high (MSI-H) status of GC, compared with microsatellite instability-low status (Fig. 1F). Using the TISIDB database the associations between YTHDF1 and molecular subtypes of GC were analyzed. The results revealed that among the molecular subtypes, a significantly higher expression of YTHDF1 in the chromosomal instability and Epstein-Barr virus (EBV) subtypes and the lowest in the genomic stability (GS) subtype (Fig. 1G). Additionally, the expression of YTHDF1 was assessed in GC cell lines and tissues. The results demonstrated that YTHDF1 was markedly upregulated in GC cell lines and GC samples compared with that in the normal gastric mucosa epithelial cell line GES-1 (Fig. 1H) and normal tissues (Fig. 1I).

Finally, the association between YTHDF1 expression and cell survival was evaluated. Kaplan-Meier analysis suggested that patients with GC with high YTHDF1 expression had significantly worse survival than those with low YTHDF1 expression (Fig. 2A). Furthermore, overexpression of YTHDF1 was linked to a significantly worse prognosis in liver cancer, thyroid carcinoma, breast cancer, ovarian cancer, and endometrial carcinoma for those with high YTHDF1 expression compared with those with low expression (Fig. 2B-F). Overall, the findings indicate that YTHDF1 is markedly upregulated and is associated with poor survival in patients with GC.

Associations between YTHDF1 and the immune infiltration level in GC. YTHDF1 overexpression was observed in MSI-H and EBV-associated GC. Considering the association between MSI-H and EBV with GC immunotherapy (35), the present study assessed the association between YTHDF1 expression and immune infiltration levels in GC. The correlation between YTHDF1 expression and TILs was evaluated using the TISIDB database. Fig. 3A shows the Spearman's correlations between YTHDF1 and TILs across 30 human tumors. Furthermore, YTHDF1 expression demonstrated a significant negative correlation with the levels of activated CD8 T cells (ρ=-0.174; P=0.00037), central memory CD8 T cells (ρ=-0.27; P=2.6x10^{-8}), effector memory CD8 T cells (ρ=-0.46; P<2.2x10^{-16}), central memory CD4 T cells (ρ=-0.302; P=3.87x10^{-10}), effector memory CD4 T cells (ρ=-0.468; P<2.2x10^{-16}), activated B cells (ρ=-0.412; P<2.2x10^{-16}), immune B cells (ρ=-0.452; P<2.2x10^{-16}), macrophages (ρ=-0.406; P<2.2x10^{-16}), activated DCs (ρ=-0.226; P=3.41x10^{-6}), monocytes (ρ=-0.211; P=1.53x10^{-5}), regulatory T cells (Tregs) (ρ=-0.3; P=5.33x10^{-10}) and myeloid-derived suppressor cells (MDSCs; ρ=-0.351; P=2.29x10^{-13}) in GC (Fig. 3B-K).

Using the TIMER database, the correlation between YTHDF1 and immune cell infiltration levels in GC were further assessed. The results revealed a significant negative correlation between YTHDF1 expression and infiltrating CD8^{+} T cells (cor=-0.187; P=2.91x10^{-4}), macrophages (cor=-0.223; P=1.45x10^{-5}), neutrophils (cor=-0.189; P=2.54x10^{-4}) and DCs (cor=-0.204; P=7.48x10^{-5}; Fig. 3L). Notably, the correlation between YTHDF1 and CD4^{+} T cells did not reach statistical significance (Fig. 3L), which differed from the results of the TISIDB database. Additionally, in response to copy number alterations in YTHDF1 cells, the infiltration levels of several immune cells were significantly decreased compared with the cells without such variations (Fig. 3M).

To further evaluate these findings in clinical GC samples, 16 GC specimens were collected to assess the expression of YTHDF1 using IHC (Fig. 4A). The specimens were categorized into the high and low YTHDF1 expression groups according to their SI scores. Subsequently, lymphocyte subset data obtained from the clinical records of each patient were analyzed. Differences between the high and low YTHDF1 expression groups concerning lymphocytes were analyzed using GraphPad Prism 8.0.2. The results demonstrated that total lymphocytes and T cells were significantly more abundant in the low YTHDF1 expression group compared with the high YTHDF1 expression group (Fig. 4B and C). Regarding the lymphocyte subsets, significantly higher levels of CD8^{+} T cells were observed in the low YTHDF1 expression group compared with that in the high YTHDF1 expression group, whereas the levels of CD4^{+} T, NK and B cells were not significantly different (Fig. 4D-G).

Correlation between YTHDF1 and immune markers. To gain further insight into the association between YTHDF1 and TILs in GC, the relationship between YTHDF1 and immune markers was analyzed. The results revealed a significant positive correlation between YTHDF1 expression and tumor associate macrophage (TAM)-related markers such as colony-stimulating factor 1, signal transducer and activator of transcription 3, signal transducer and activator of transcription 6 and CD274 [programmed death-ligand 1 (PD-L1); Fig. 5A]. Conversely, markers associated with DC demonstrated a significantly negative correlation with YTHDF1 expression
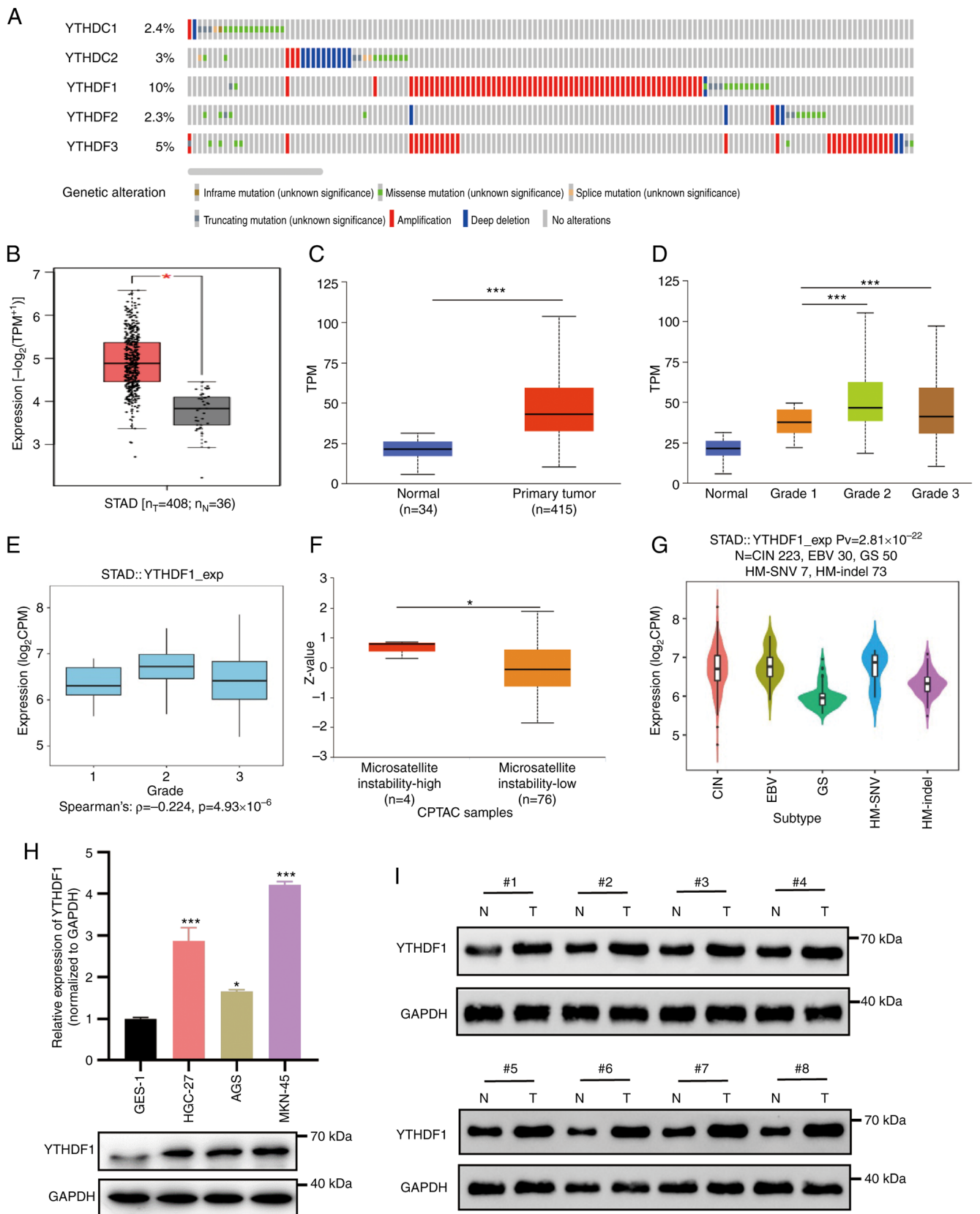
Figure 1. YTHDF1 expression in GC is elevated and associated with pathological features. (A) Genetic alterations in the YTH domain family in GC were analyzed using the cBioPortal database. YTHDF1 was overexpressed in GC tissue compared with adjacent normal tissue analyzed with the (B) Gene expression profiling interactive analysis and (C) University of Alabama at Birmingham Cancer data analysis portal databases. (D) YTHDF1 expression was associated with tumor grade in GC analyzed by UALCAN database. (E) YTHDF1 expression was associated with tumor grade in GC analyzed by TISIDB database (F) YTHDF1 expression was associated with microsatellite status in GC. (G) Associations between YTHDF1 and molecular subtypes in GC were analyzed using the Tumor-immune system interactions and drug bank database. (H) YTHDF1 expression in GC cell lines was analyzed using reverse transcription-quantitative PCR. (I) Differences in YTHDF1 expression between GC and paired normal tissue was analyzed using western blotting. [*]P<0.05; [***]P<0.001. YTHDF1, YTH N[6]-methyladenosine RNA binding protein 1; GC, gastric cancer; STAD, stomach adenocarcinoma; T, tumor; N, normal; TPM, transcript per million; CPM, counts per million reads; CPTAC, Clinical Proteomic Tumor Analysis Consortium; PCR, polymerase chain reaction.
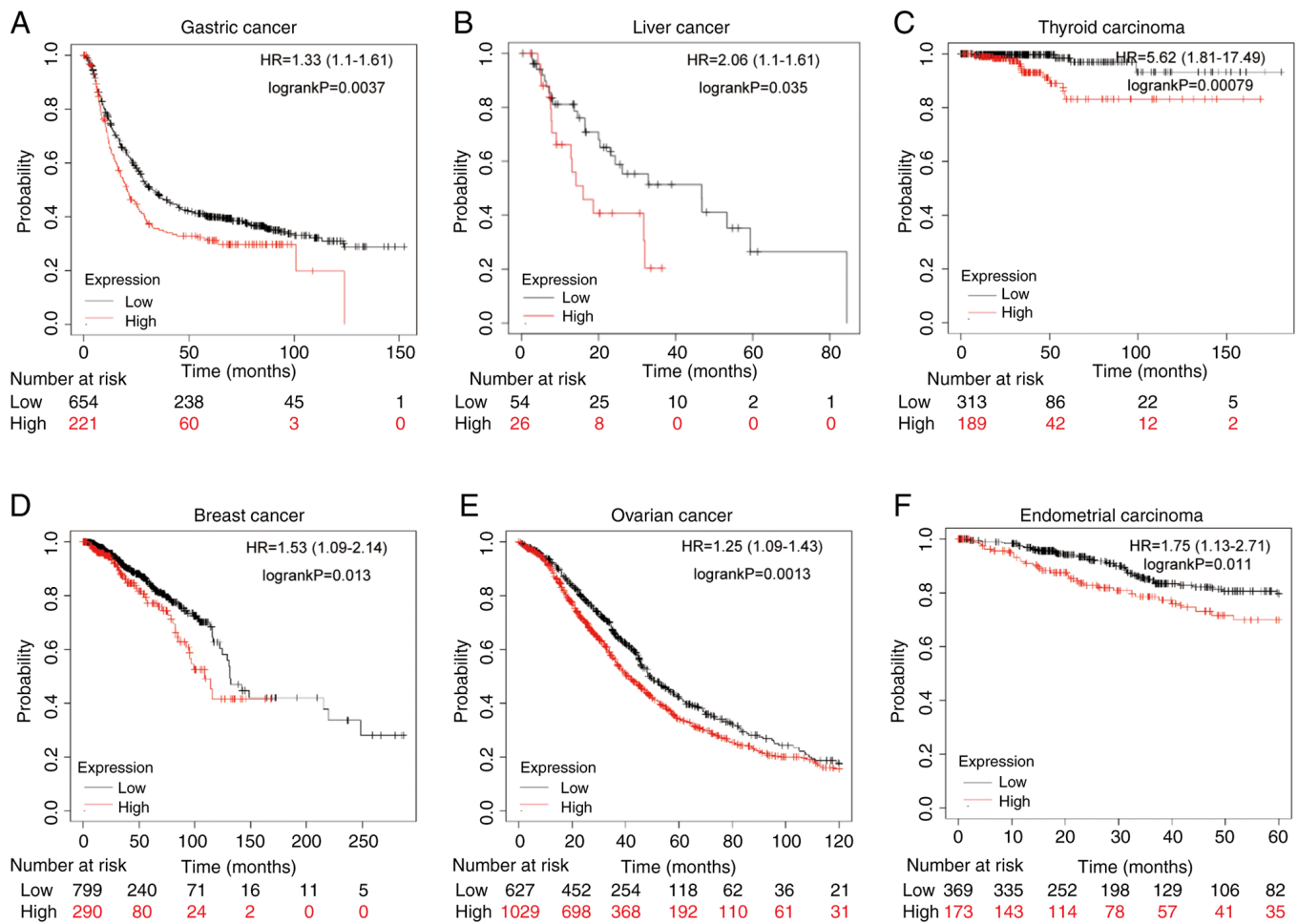
Figure 2. Prognostic value of YTHDF1 in different types of human cancers. Kaplan-Meier analysis suggested that upregulation of YTHDF1 indicates poor prognosis in patients with (A) gastric, (B) liver, (C) thyroid, (D) breast, (E) ovarian cancers and (F) endometrial carcinoma. YTHDF1, YTH N[6]-methyladenosine RNA binding protein 1; HR, hazard ratio.

(Fig. 5B). Additionally, a significant positive correlation was observed between YTHDF1 and Treg markers (Fig. 5C-E) and T cell exhaustion markers (Fig. 5F-H).

YTHDF1 interacts with p53. To assess the mechanism of YTHDF1 in GC, the association between YTHDF1 and GC-related gene expression was first evaluated. The results indicated a significant positive correlation between YTHDF1 expression and p53 (R=0.38; P<0.0001; Fig. 6A), HER-2 (R=0.21; P=6.7x10^{-8}; Fig. 6B) and KRAS (R=0.21; P=9.1x10^{-8}; Fig. 6C), with p53 exhibiting the strongest correlation with YTHDF1 expression. As p53 is a tumor suppressor gene and mutant p53 acts as an oncogene (36), the differential expression of YTHDF1 between GC with wild-type p53 and with mutant p53 was also assessed. These results suggested that YTHDF1 was significantly upregulated in GC with mutant p53 compared with GC with wild-type p53 (Fig. 6D). Furthermore, immune infiltration levels were significantly downregulated in GC with mutant p53 compared with GC with wild-type p53 (Fig. 6E).

Subsequently, the protein-protein interactions of YTHDF1 were evaluated. First, the GeneMANIA database was used to determine the interaction between YTHDF1 and p53. The results revealed interactions between YTHDF1 and p53,

p21 and MDM2 (Fig. 6F). The HitPredict database further confirmed the interaction between YTHDF1 and p53 with high confidence, with an interaction score of 0.479 (Fig. 6G).

Furthermore, the transfection efficiency of plasmids overexpressing p53 or YTHDF1 in 293T cells through RT-qPCR and WB experiments (Fig. S1). Subsequently, co-immunoprecipitation assays were performed to confirm the interaction between YTHDF1 and p53. The results revealed that Myc-YTHDF1 co-immunoprecipitated with p53 using an anti-p53 antibody, and p53 co-immunoprecipitated with Myc-YTHDF1 using an anti-Myc antibody (Fig. 6H and I). These results suggest that p53 is a potential target of YTHDF1.

Enrichment analysis of YTHDF1 functional networks in GC. The LinkedOmics database was used to assess the YTHDF1 mRNA sequence in GC. Genes that were positively and negatively correlated with YTHDF1 are depicted in a volcano plot (Fig. 7A). The top 50 significantly differentially expressed genes are presented in Fig. 7B and C. Subsequently, KEGG and Gene Ontology analyses were performed using these related genes. The KEGG analysis suggested that YTHDF1 was associated with DNA replication, RNA transport, mismatch repair and the cell cycle (Fig. 7D). Cellular component analysis suggested that YTHDF1 was associated with
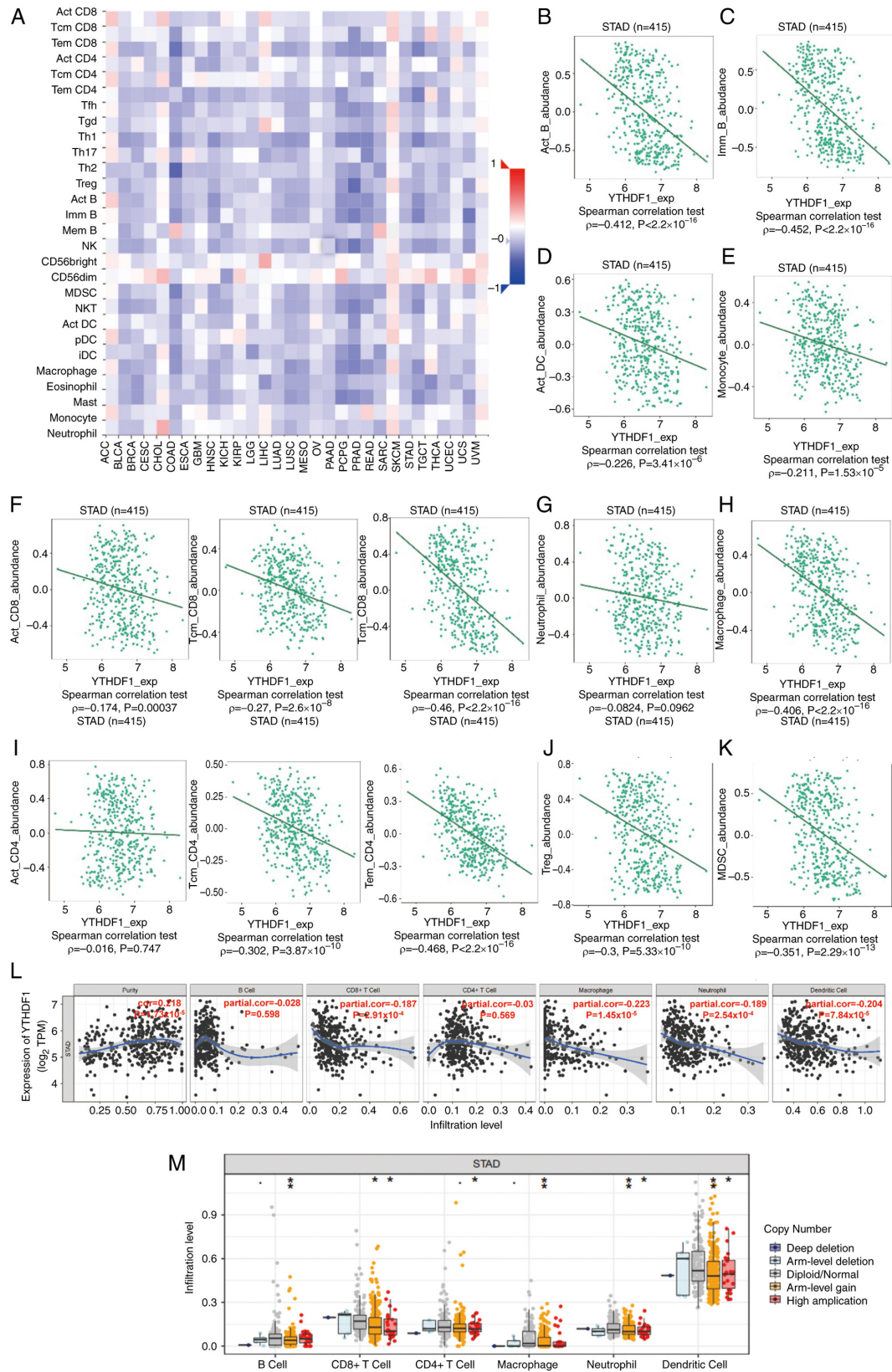
Figure 3. Correlation between YTHDF1 expression and immune infiltration level. (A) Spearman's correlations between YTHDF1 expression and TILs across several human cancer types. Correlations between YTHDF1 expression and specific immune cell types in gastric cancer, including (B) B cells, (C) macrophages, (D) DCs, (E) monocytes, (F) CD8+ T cells, (G) neutrophils, (H) Tregs, (I) CD4+ T cells, (J) Treg cells and (K) MDSC cells, were analyzed using the Tumor-Immune System Interactions and Drug Bank database. (L) Correlation between YTHDF1 expression and immune infiltration levels in gastric cancer was analyzed using the TIMER database. (M) Comparison of immune infiltration levels between gastric cancer with or without YTHDF1 copy number alterations was performed using the SCNA module of the TIMER database. *P<0.05; **P<0.01. YTHDF1, YTH N[6]-methyladenosine RNA binding protein 1; TILs, tumor-infiltrating lymphocytes; DCs, dendritic cells; Tregs, regulatory T cells; MDSCs, myeloid-derived suppressor cells; TIMER, Tumor Immune Estimation Resource; STAD, stomach adenocarcinoma; Act_CD8, activated CD8 T cells; Tcm_CD8, central memory CD8 T cells; Tem_CD8, effector memory CD8 T cells; Tcm_CD4, central memory CD4 T cells; Tem_CD4, effector memory CD4 T cells; Act_B, activated B cells; Imm_B, immune B cells; TPM, transcripts per million.
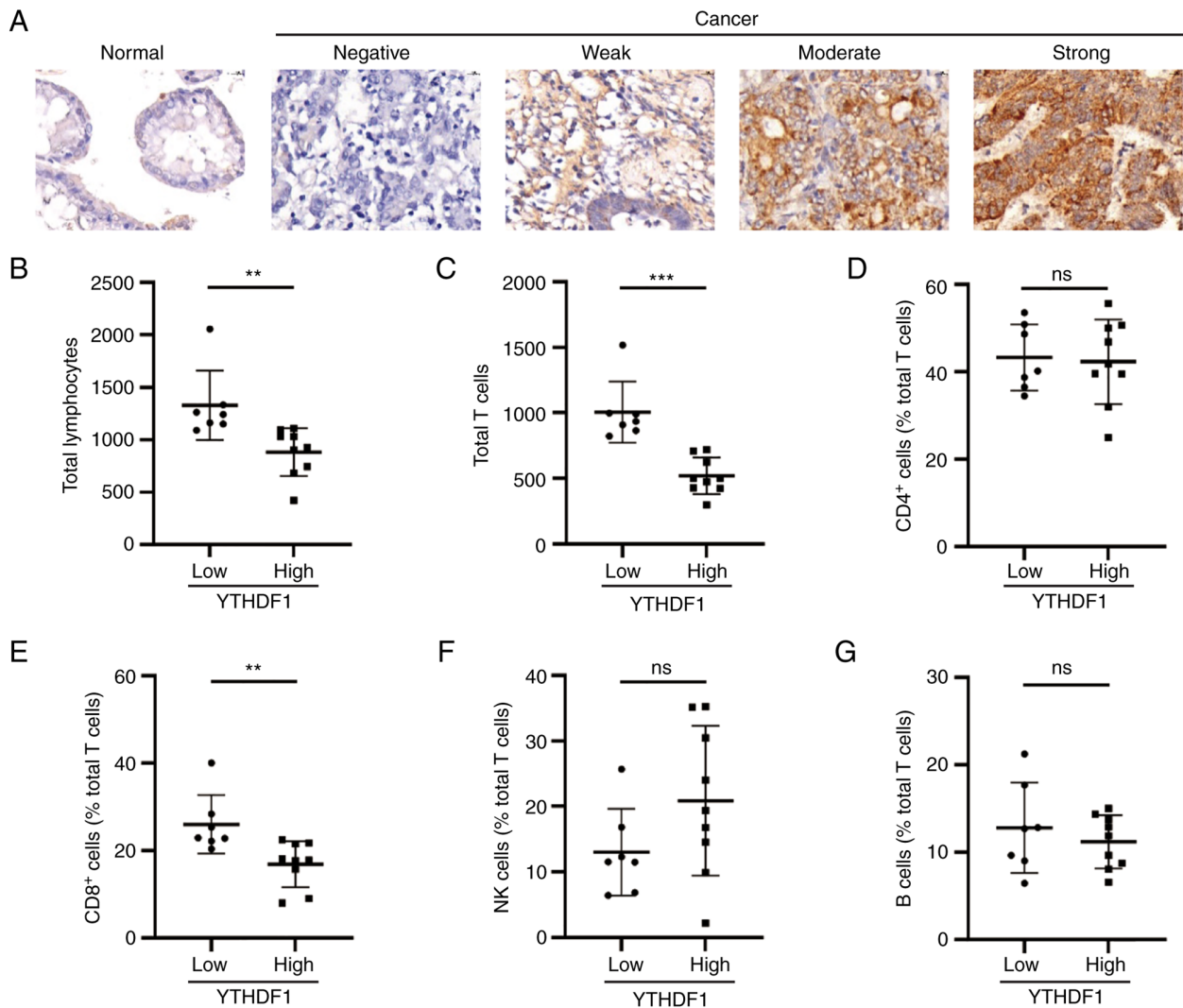
Figure 4. Lymphocyte subsets enrichment in GC specimens. (A) Representative immunohistochemistry images of different YTHDF1 expression levels in GC specimens (x100 magnification, stained with liquid DAB). Difference in the lymphocyte subsets infiltration level in GC specimens with high and low levels of YTHDF1 expression: (B) Total lymphocyte, (C) total T cell, (D) CD4+ T cell, (E) CD8+ T cell, (F) NK cell and (G) B cell. **$P<0.01$; ***$P<0.001$. GC, gastric cancer; YTHDF1, YTH N^6-methyladenosine RNA binding protein 1; NK, natural killer; ns, not significant.

condensed chromosomes, methyltransferase complexes, replication forks, acetyltransferase complexes, DNA packaging complexes, protein-DNA complexes and ATPase complexes (Fig. 7E). Biological process analysis revealed that YTHDF1 was associated with non-coding (nc)RNA processing, mRNA processing, chromosome segregation, transfer RNA metabolic processes, ribosomal RNA metabolic processes, RNA localization, meiotic cell cycle, DNA replication and cell cycle checkpoints (Fig. 7F). Molecular function analysis demonstrated that YTHDF1 was associated with catalytic activity, acting on DNA, catalytic activity, acting on RNA, helicase activity, nucleotidyltransferase activity, ATPase activity, ribonucleoprotein complex binding, telomerase RNA binding, RNA polymerase binding, ubiquitin-like protein binding and histone binding (Fig. 7G).

Discussion

The m6A reader YTHDF1 has been assessed in several types of human tumors; however, the role of YTHDF1 in GC remains unclear. In the present study, the expression of YTHDF1 in GC was evaluated, and the results suggest that YTHDF1 is upregulated in GC, demonstrating an association with tumor grade, microsatellite status and molecular subtype. Furthermore, the association between YTHDF1 and the immune microenvironment was assessed. The findings revealed that the infiltration levels of many TIL subsets were significantly lower in GC with high YTHDF1 expression than in GC with low YTHDF1 expression. Conversely, the levels of markers associated with T cell exhaustion were significantly higher. Mechanistically, high YTHDF1 expression was strongly associated with p53 mutations. Protein-protein interaction analysis revealed an interaction between YTHDF1 and p53. Therefore, we hypothesize that YTHDF1 regulates immune cell infiltration in GC through its interaction with p53.

The avoidance of immune destruction is a hallmark of cancer (37). Alteration of the TME is an important mechanism through which tumors evade immunity (38). Several studies have reported an association between changes in immune cell infiltration and tumor formation, progression, prognosis and
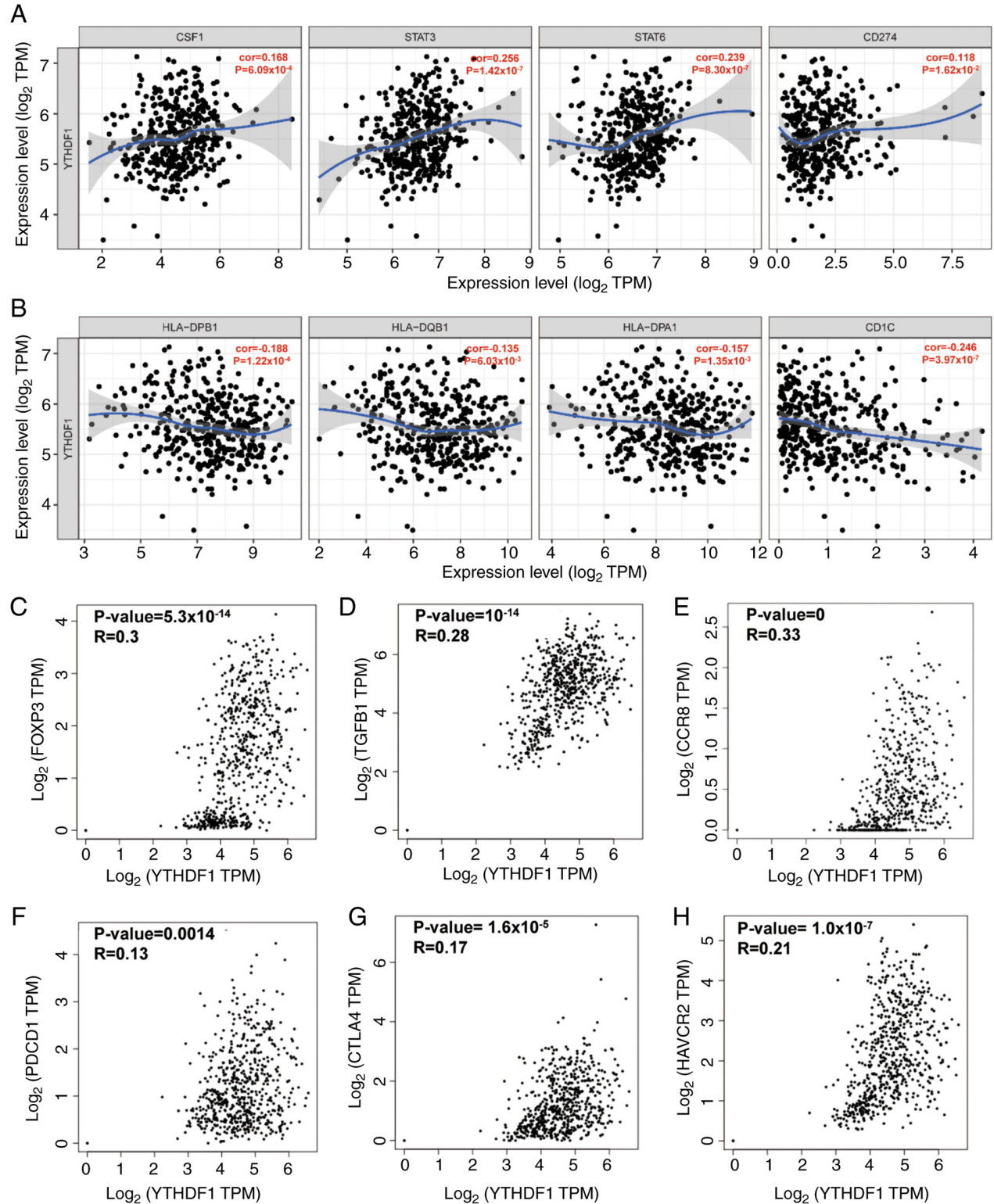
Figure 5. Correlation between YTHDF1 and markers of immune cells in gastric cancer. Correlation between YTHDF1 and (A) tumor associate macrophage-related genes and markers and (B) DC markers were analyzed using the Gene module of the Tumor Immune Estimation Resource database. Correlation between YTHDF1 and Treg markers, including (C) Foxp3, (D) TGFB1 and (E) CCR8 were analyzed using the GEPIA database. Correlation between YTHDF1 and T cell exhaustion markers, namely (F) PDCD1, (G) CTLA4 and (H) HAVCR2 (T cell immunoglobulin and mucin-domain-containing-3) were analyzed using the GEPIA database. YTHDF1, YTH N^6-methyladenosine RNA binding protein 1; CSF1, colony-stimulating factor 1; STAT, signal transducer and activator of transcription; TPM, transcripts per million; DC, dendritic cell; Foxp3, forkhead box P3; TGFB1, transforming growth factor-β1; CCR8, C-C motif chemokine receptor; PDCD1, programmed cell death 1; CTLA-4, T-lymphocyte-associated protein 4; HAVCR2, hepatitis A virus cellular receptor 2; GEPIA, Gene Expression Profiling Interactive Analysis.

overall immune response. The upregulation of certain oncogenes or downregulation of tumor suppressor genes may affect tumor occurrence and development by altering the TME and immune cell infiltration (17,39). Qi *et al* (40) reported that in
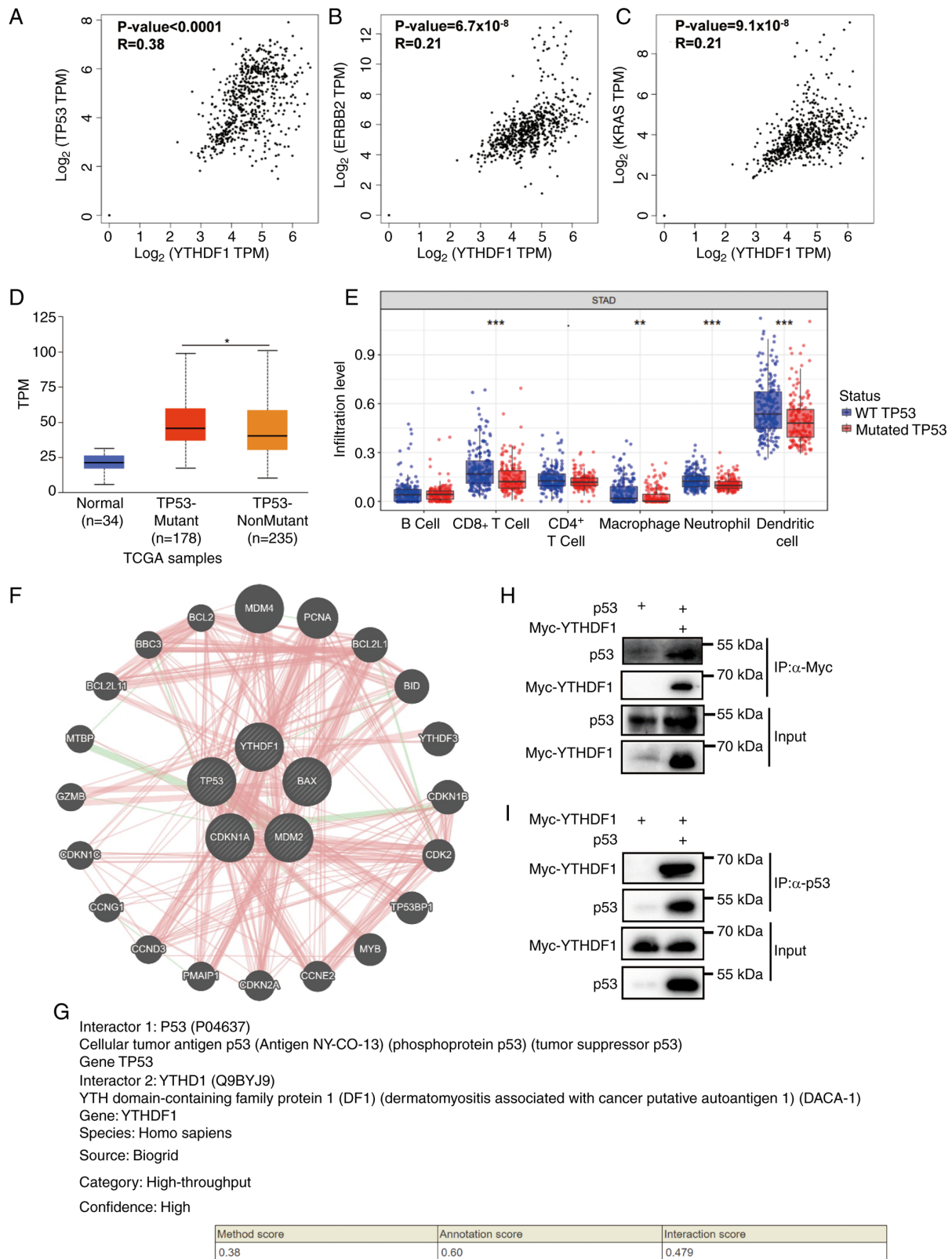
Figure 6. Interactions between YTHDF1 and p53. Correlation between YTHDF1 and the gastric-related genes (A) TP53, (B) ERBB2 (HER-2) and (C) KRAS were analyzed using the Gene Expression Profiling Interactive Analysis database. (D) YTHDF1 expression was elevated in TP53 mutant gastric cancer compared with TP53 nonmutant gastric cancer, as analyzed using the University of Alabama at Birmingham Cancer data analysis portal database. (E) TP53 mutation was associated with decreased immune cell infiltration levels in gastric cancer, as analyzed by the Tumor Immune Estimation Resource database. (F) p53 interaction with YTHDF1 was analyzed using the GeneMANIA database. (G) p53 interaction with YTHDF1 was analyzed using the HitPredict database. (H) Interactions between YTHDF1 and p53 were assessed using immunoprecipitation assays in 293T cells transfected with plasmids, followed by co-immunoprecipitation assays using anti-Myc antibodies. (I) Interactions between YTHDF1 and p53 were assessed using immunoprecipitation assays in 293T cells transfected with plasmids, followed by co-immunoprecipitation assays using anti-p53 antibodies. $^{*}P<0.05$; $^{**}P<0.01$; $^{***}P<0.001$. YTHDF1, YTH N^{6}-methyladenosine RNA binding protein 1; TP53, tumor protein p53; ERBB2, erb-b2 receptor tyrosine kinase 2; HER-2, human epidermal growth factor receptor-2; KRAS, KRAS proto-oncogene; TPM, transcripts per million; TCGA, The Cancer Genome Atlas; WT, wild type; STAD, stomach adeno-carcinoma.
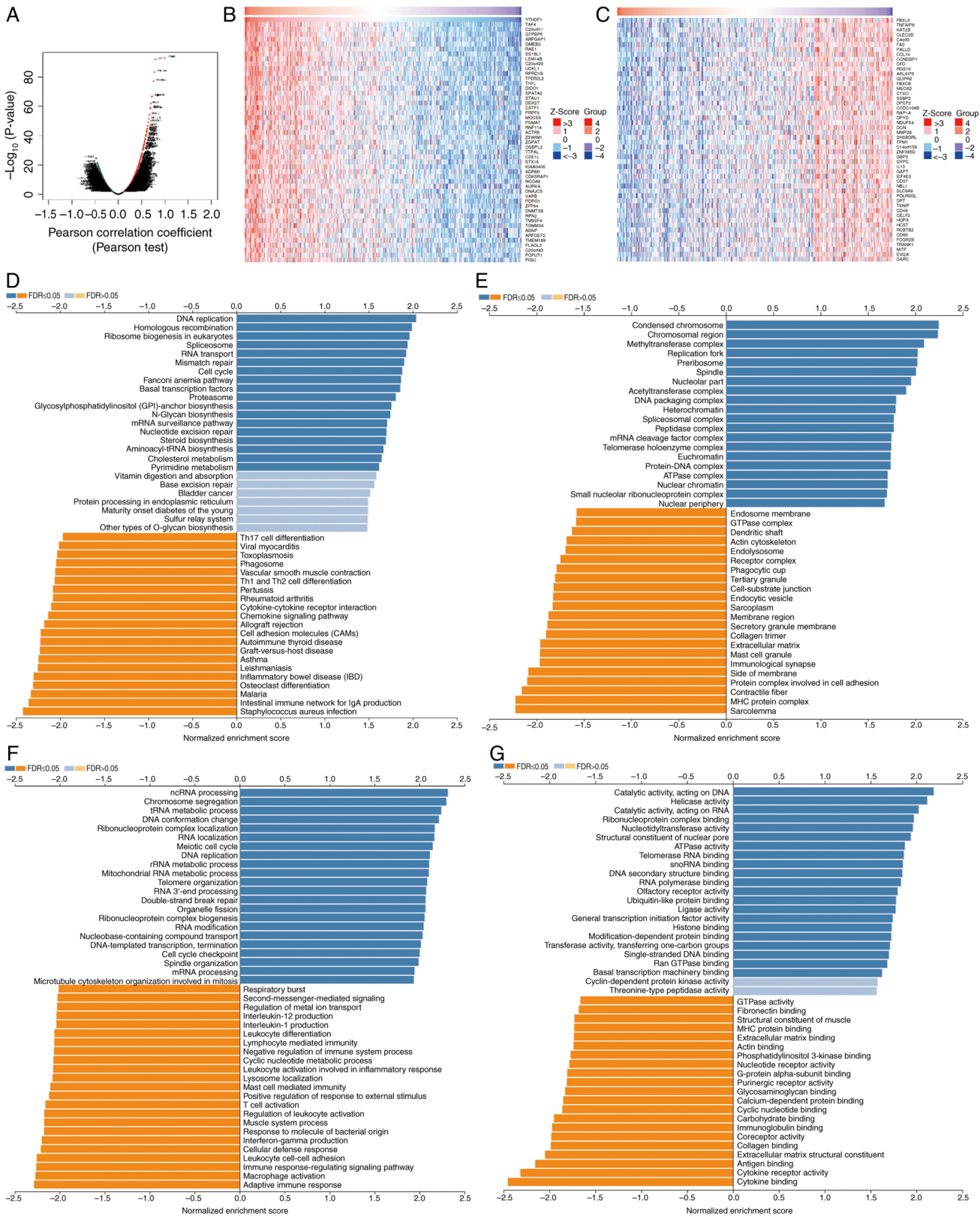
Figure 7. Enrichment analysis of YTHDF1 functional networks in gastric cancer using the LinkedOmics database. (A) Volcano plot illustrating upregulated (red) and downregulated (green) genes. Heatmap showing the top 50 genes (B) positively associated with YTHDF1 and (C) negatively associated with YTHDF1. (D) KEGG analysis, (E) cellular component analysis, (F) biological process analysis and (G) molecular function analysis of YTHDF1 was performed using the Gene Set Enrichment Analysis tool. YTHDF1, YTH N^6-methyladenosine RNA binding protein 1; FDR, false discovery rate; KEGG, Kyoto Encyclopedia of Genes and Genomes.

an hepatocellular carcinoma cohort with improved survival, immune cells were enriched in both tumors and normal

tissues. Moreover, the density of PD-L1-expressing tumor cells was higher in this cohort, which may benefit more from PD-1

treatment (40). In addition, anticancer treatments can remodel the TIME. Zetrini *et al* (41) used the bioreactivity of novel polymer-lipid manganese dioxide nanoparticles (PLMDs) to remodel the TIME. The study reported that intravenous injection of PLMDs suppressed the recruitment of Tregs and MDSCs, whilst radiation alone enhanced these processes. Pretreatment with PLMDs followed by radiation downregulated programmed death ligand 1 and promoted the infiltration of antitumor CD8$^+$ T cells and M1 macrophages into tumor sites (41). Furthermore, a recent bioinformatics analysis constructed a risk model based on eight necrosis-related long non-coding (lnc)RNAs [all eight lncRNAs were highly expressed in patients with esophageal carcinoma (ESCA)], which divided patients with ESCA into high- and low-risk groups based on their scores. Analysis of the relationship between risk score and immune cell infiltration revealed that the high-risk group had more abundant neutrophils and Th2 cells, whereas the low-risk group had more abundant macrophages and NK cells. Furthermore, most immune checkpoints (TNFRSF18, BTNL2, CD276, CD40, CD86, CD44 and TNFSF18) were more activated in the low-risk group (42). In the present study, a significant reduction in immune cell infiltration was observed in the YTHDF1 expression group. YTHDF1 demonstrated a negative correlation with antitumor CD8$^+$ T cells, macrophages and NK cells, but a positive correlation with immune suppressor markers related to TAM and Treg markers. Collectively, these findings, along with prior research, underscore the important role of the TME and immune cell infiltration in tumors.

YTHDF1 has been confirmed to be an oncogene in specific types of human tumors and is associated with a poor prognosis. Liu *et al* (14) reported that YTHDF1 is overexpressed in ovarian cancer, and patients with high YTHDF1 expression experienced shorter survival. Mechanistically, YTHDF1 enhances eukaryotic initiation factor 3C (EIF3C) translation by binding to the m6A site of EIF3C mRNA, thereby facilitating the tumorigenesis and metastasis of ovarian cancer (14). Similarly, YTHDF1 enhances forkhead box protein M1 (FOXM1) translation by recognizing and binding to the m6A-modified FOXM1 mRNA, which promotes breast cancer metastasis and leads to shorter survival (43). Similar results have been observed for GC. Pi *et al* (44) suggested that YTHDF1 is highly expressed in GC and associated with poor survival, and further showed that YTHDF1 hyperactivates the Wnt/β-catenin pathway by enhancing the translation of frizzled 7, a key Wnt signaling receptor, leading to stomach carcinogenesis (44). Another study reported that YTHDF1 enhances ubiquitin-specific protease 14 translation, thus promoting GC carcinogenesis and metastasis (45). The present study demonstrated that YTHDF1 is the m6A reader with the highest mutation frequency and is highly expressed in GC tissues. Survival analysis suggested that patients with high YTHDF1 expression had a poor prognosis. This is consistent with previous studies and confirms the carcinogenic role of YTHDF1 in GC. However, the precise role of YTHDF1 in GC remains unclear.

Previous studies have demonstrated the association of YTHDF1 with immune cell infiltration in different tumor types. Liu *et al* (46) reported a positive correlation between YTHDF1 and B cells and macrophages in esophageal

carcinomas. Tsuchiya *et al* (47) assessed the relationship between YTHDF1 expression and four TIL subsets (PD-1$^+$, CD8$^+$, Foxp3$^+$ and CD45RO$^+$) in non-small cell lung cancer. Their findings suggested that the TIL levels of the four lymphocyte subsets were strongly upregulated in high YTHDF1- and YTHDF2-expressing tumors (47). Contrary to these results, the present study demonstrated a negative association between YTHDF1 and CD8$^+$ T cells, macrophages, neutrophils, central memory CD4$^+$ T cells, effector memory CD4$^+$ T cells and activated B cells. Immune cell infiltration was significantly reduced in GC cells with high YTHDF1 expression. Furthermore, YTHDF1 copy number alteration downregulated the infiltration levels of immune cells. Han *et al* (48) reported an association between YTHDF1 and DCs, demonstrating that YTHDF1 regulates durable neoantigen-specific immunity in YTHDF1 wild type mice. In classical DCs, deletion of YTHDF1 increases the cross-presentation of tumor antigens. In addition, the loss of YTHDF1 enhances cross-priming of CD8$^+$ T cells (48). Furthermore, in gastric cancers, YTHDF1 is associated with DCs. Bai *et al* (49) reported that YTHDF1-knockout in GC led to recruitment of mature DCs and enhanced the infiltration of CD4$^+$ and CD8$^+$ T cells (49). In the present study, YTHDF1 expression demonstrated a negative correlation with the number of DCs in GC. Levels of dendritic cell markers were significantly lower in gastric cells with high YTHDF1 expression. This finding is consistent with previous studies demonstrating the immunosuppressive effect of YTHDF1 in GC.

Tregs, which are essential for maintaining T cell tolerance to autoantigens and inhibiting T cell immunity to tumor-associated antigens, are a population of T cells that functionally inhibit immune responses by affecting the activity of other cell types (50). Tregs represent a population of CD4$^+$CD25$^+$FOXP3$^+$ T cells derived from the thymus. High Treg infiltration is markedly associated with unfavorable outcomes across several human cancer types (51-54). The transcription factor FOXP3 is the most important marker of Tregs and aids in their identification (55). The results from the present study suggest a positive association between YTHDF1 and FOXP3 expression. Furthermore, YTHDF1 was positively associated with other Treg markers, such as transforming growth factor-β1 and C-C motif chemokine receptor. These findings suggest that YTHDF1 may contribute to poor prognosis in GC by upregulating Treg infiltration.

T-cell exhaustion is a state of T-cell dysfunction, characterized by continuous expression of inhibitory receptors and leading to reduced cytokine secretion and effector function. These inhibitory receptors include programmed cell death 1, cytotoxic T-lymphocyte associated protein 4 (CTLA4), and hepatitis A virus cellular receptor 2 (also known as T cell immunoglobulin and mucin-domain-containing-3; TIM-3). Several studies have reported that T-cell exhaustion is linked to poor prognosis and immunotherapy response (56,57). Therefore, reversing T-cell exhaustion has become an important method in tumor immunotherapy (58). In the present study, a significant increase in the expression of inhibitory receptors PD-1, CTLA4 and TIM-3 was demonstrated in GC cells with high YTHDF1 expression, indicating that YTHDF1 may promote the expression of these inhibitory receptors. Therefore, targeting YTHDF1 may reverse the T cell exhaustion status,

which would provide a new target for improving the response to immunotherapy in GC.

p53 is an important tumor suppressor and is closely related to the immune microenvironment (39). Several studies have reported that YTHDF1 expression is associated with p53 expression. Li *et al* (18) reported that YTHDF1 and heterogeneous nuclear ribonucleoprotein A2/B1 inhibit the role of p53 in suppressing carcinogenesis and melanoma development by upregulating genes involved in the p53 signaling pathway. Zhao *et al* (59) reported that YTHDF1 increased the expression of Yin-Yang 1 and MDM2, two negative p53 regulators, by increasing their transcription levels; this led to the inhibition of p53 activity to regulate arsenite-induced human keratinocyte transformation (59). Furthermore, in hepatocellular carcinoma, YTHDF1 expression and the p53 signaling pathway were correlated (15). In the present study, a positive association was demonstrated between YTHDF1 and p53 expression in GC. Furthermore, compared with p53 wild-type GC, YTHDF1 expression was significantly increased, and the level of immune cell infiltration was significantly reduced in p53 mutant GC. Protein-protein interaction analysis confirmed the interaction between YTHDF1 and p53. Previous studies have reported that genetic alterations in m6A regulators, including METTL3/14, YTHDF1, YTHDF2, FTO and ALKBH5, strongly correlate with p53 mutations (60,61). Therefore, we hypothesize that YTHDF1 interacts with mutant p53 in GC. Enrichment analysis revealed the association between YTHDF1 with DNA replication, RNA transport, mismatch repair, cell cycle and ncRNA processing - all of which are also related to p53. Activating p53 is an important strategy in tumor treatment (62). Based on the results of the present study, selecting appropriate p53 agonists by detecting the expression status of YTHDF1 may enhance the antitumor effect of p53 agonists, and this may be a potential strategy for improving the efficacy of gastric cancer immunotherapy. In addition, the present study revealed a positive correlation between YTHDF1, KRAS and HER-2. However, no previous studies have explored this association, to the best of our knowledge. Both KRAS and HER-2 serve crucial roles as therapeutic targets in the occurrence and development of GC (63); however, further investigation is required to determine whether YTHDF1, KRAS and HER-2 are involved in the progression of GC.

Whilst this study exhibits promising potential, it also presents certain limitations. Most of the results in the present study are obtained from online database analyses, and although they have been partially validated through small clinical samples, further cellular and animal experiments should be performed in the future to verify the findings. Additionally, in terms of mechanisms of action, the present study identified that YTHDF1 can bind to p53, yet the specific regulatory mechanisms remain elusive. We hypothesize that there are several possible mechanisms: YTHDF1 regulates the expression of downstream target genes by binding to p53; YTHDF1 affects the activity of the p53 pathway by binding to p53, thereby interactively regulating signaling pathways related to tumor immunity; YTHDF1 influences the methylation level of p53 by binding to it; and upstream targets affect the interaction between YTHDF1 and p53. Further *in vitro* and *in vivo* experiments are required to validate these regulatory mechanisms.

In conclusion, the present study confirmed that YTHDF1 is associated with a poor prognosis. We hypothesize, for the first time to the best of our knowledge, that YTHDF1 regulates immune cell infiltration by interacting with p53 in GC, providing a promising direction for future research.

Availability of data and materials

The data generated in the present study may be requested from the corresponding author.

Authors' contributions

QL designed the study, performed the data analysis and wrote the manuscript. JX conceived and designed the study, and revised the manuscript. All authors have reviewed and approved the final manuscript. QL and JX confirm the authenticity of all the raw data.

Ethics approval and consent to participate

The present study was approved by the Ethics Committee of the First Affiliated Hospital of Nanchang University [2023; approval no. CDYFYYLK(03-011)]. All patients provided signed informed consent before sample collection.

Patient consent for publication

Not applicable.

Competing interests

The authors declare that they have no competing interests.

References

1. Joshi SS and Badgwell BD: Current treatment and recent progress in gastric cancer. CA Cancer J Clin 71: 264-279, 2021.
2. Sung H, Ferlay J, Siegel RL, Laversanne M, Soerjomataram I, Jemal A and Bray F: Global Cancer statistics 2020: GLOBOCAN estimates of incidence and mortality worldwide for 36 cancers in 185 countries. CA Cancer J Clin 71: 209-249, 2021.
3. Gong J, Chehrazi-Raffle A, Reddi S and Salgia R: Development of PD-1 and PD-L1 inhibitors as a form of cancer immunotherapy: A comprehensive review of registration trials and future considerations. J Immunother Cancer 6: 8, 2018.
4. Desrosiers R, Friderici K and Rottman F: Identification of methylated nucleosides in messenger RNA from Novikoff hepatoma cells. Proc Natl Acad Sci USA 71: 3971-3975, 1974.
5. Zaccara S, Ries RJ and Jaffrey SR: Reading, writing and erasing mRNA methylation. Nat Rev Mol Cell Biol 20: 608-624, 2019.
6. Wang L, Hui H, Agrawal K, Kang Y, Li N, Tang R, Yuan J and Rana TM: m6A RNA methyltransferases METTL3/14 regulate immune responses to anti-PD-1 therapy. EMBO J 39: e104514, 2020.

7. Huang H, Wang Y, Kandpal M, Zhao G, Cardenas H, Ji Y, Chaparala A, Tanner EJ, Chen J, Davuluri RV and Matei D: FTO-dependent N 6-methyladenosine modifications inhibit ovarian cancer stem cell self-renewal by blocking cAMP signaling. Cancer Res 80: 3200-3214, 2020.
8. Tang B, Yang Y, Kang M, Wang Y, Wang Y, Bi Y, He S and Shimamoto F: m6A demethylase ALKBH5 inhibits pancreatic cancer tumorigenesis by decreasing WIF-1 RNA methylation and mediating Wnt signaling. Mol Cancer 19: 3, 2020.
9. Xiao W, Adhikari S, Dahal U, Chen YS, Hao YJ, Sun BF, Sun HY, Li A, Ping XL, Lai WY, et al: Nuclear m6A reader YTHDC1 regulates mRNA splicing. Mol Cell 61: 507-519, 2016.
10. Wojtas MN, Pandey RR, Mendel M, Homolka D, Sachidanandam R and Pillai RS: Regulation of m6A transcripts by the 3'→5' RNA helicase YTHDC2 is essential for a successful meiotic program in the mammalian germline. Mol Cell 68: 374-387.e12, 2017.
11. Zhang C, Huang S, Zhuang H, Ruan S, Zhou Z, Huang K, Ji F, Ma Z, Hou B and He X: YTHDF2 promotes the liver cancer stem cell phenotype and cancer metastasis by regulating OCT4 expression via m6A RNA methylation. Oncogene 39: 4507-4518, 2020.
12. Chang G, Shi L, Ye Y, Shi H, Zeng L, Tiwary S, Huse JT, Huo L, Ma L, Ma Y, et al: YTHDF3 induces the translation of m6A-enriched gene transcripts to promote breast cancer brain metastasis. Cancer Cell 38: 857-871.e7, 2020.
13. Jia R, Chai P, Wang S, Sun B, Xu Y, Yang Y, Ge S, Jia R, Yang YG and Fan X: m6A modification suppresses ocular melanoma through modulating HINT2 mRNA translation. Mol Cancer 18: 161, 2019.
14. Liu T, Wei Q, Jin J, Luo Q, Liu Y, Yang Y, Cheng C, Li L, Pi J, Si Y, et al: The m6A reader YTHDF1 promotes ovarian cancer progression via augmenting EIF3C translation. Nucleic Acids Res 48: 3816-3831, 2020.
15. Zhao X, Chen Y, Mao Q, Jiang X, Jiang W, Chen J, Xu W, Zhong L and Sun X: Overexpression of YTHDF1 is associated with poor prognosis in patients with hepatocellular carcinoma. Cancer Biomark 21: 859-868, 2018.
16. Hu Y, Pan Q, Wang M, Ai X, Yan Y, Tian Y, Jing Y, Tang P and Jiang J: m6A RNA methylation regulator YTHDF1 correlated with immune microenvironment predicts clinical outcomes and therapeutic efficacy in breast cancer. Front Med (Lausanne) 8: 667543, 2021.
17. Wang Q, Zhang Q, Li Q, Zhang J and Zhang J: Clinicopathological and immunological characterization of RNA m6A methylation regulators in ovarian cancer. Mol Genet Genomic Med 9: e1547, 2021.
18. Li T, Gu M, Deng A and Qian C: Increased expression of YTHDF1 and HNRNPA2B1 as potent biomarkers for melanoma: A systematic analysis. Cancer Cell Int 20: 239, 2020.
19. Gao J, Aksoy BA, Dogrusoz U, Dresdner G, Gross B, Sumer SO, Sun Y, Jacobsen A, Sinha R, Larsson E, et al: Integrative analysis of complex cancer genomics and clinical profiles using the cBio-Portal. Sci Signal 6: pl1, 2013.
20. Huang KK, Ramnarayanan K, Zhu F, Srivastava S, Xu C, Tan ALK, Lee M, Tay S, Das K, Xing M, et al: Genomic and epigenomic profiling of high-risk intestinal metaplasia reveals molecular determinants of progression to gastric cancer. Cancer Cell 33: 137-150.e5, 2018.
21. Wang K, Yuen ST, Xu J, Lee SP, Yan HH, Shi ST, Siu HC, Deng S, Chu KM, Law S, et al: Whole-genome sequencing and comprehensive molecular profiling identify new driver mutations in gastric cancer. Nat Genet 46: 573-582, 2014.
22. Cancer Genome Atlas Research Network: Comprehensive molecular characterization of gastric adenocarcinoma. Nature 513: 202-209, 2014.
23. Kakiuchi M, Nishizawa T, Ueda H, Gotoh K, Tanaka A, Hayashi A, Yamamoto S, Tatsuno K, Katoh H, Watanabe Y, et al: Recurrent gain-of-function mutations of RHOA in diffuse-type gastric carcinoma. Nat Genet 46: 583-587, 2014.
24. Wang K, Kan J, Yuen ST, Shi ST, Chu KM, Law S, Chan TL, Kan Z, Chan AS, Tsui WY, et al: Exome sequencing identifies frequent mutation of ARID1A in molecular subtypes of gastric cancer. Nat Genet 43: 1219-1223, 2011.
25. Li T, Fan J, Wang B, Traugh N, Chen Q, Liu JS, Li B and Liu XS: TIMER: A web server for comprehensive analysis of tumor-infiltrating immune cells. Cancer Res 77: e108-e110, 2017.
26. Chandrashekar DS, Bashel B, Balasubramanya SAH, Creighton CJ, Ponce-Rodriguez I, Chakravarthi BVSK and Varambally S: UALCAN: A portal for facilitating tumor subgroup gene expression and survival analyses. Neoplasia 19: 649-658, 2017.
27. Ru B, Wong CN, Tong Y, Zhong JY, Zhong SSW, Wu WC, Chu KC, Wong CY, Lau CY, Chen I, et al: TISIDB: An integrated repository portal for tumor-immune system interactions. Bioinformatics 35: 4200-4202, 2019.
28. Lánczky A and Győrffy B: Web-based survival analysis tool tailored for medical research (KMplot): Development and implementation. J Med Internet Res 23: e27633, 2021.
29. Tang Z, Li C, Kang B, Gao G, Li C and Zhang Z: GEPIA: A web server for cancer and normal gene expression profiling and interactive analyses. Nucleic Acids Res 45: W98-W102, 2017.
30. Warde-Farley D, Donaldson SL, Comes O, Zuberi K, Badrawi R, Chao P, Franz M, Grouios C, Kazi F, Lopes CT, et al: The GeneMANIA prediction server: Biological network integration for gene prioritization and predicting gene function. Nucleic Acids Res 38: W214-W220, 2010.
31. Patil A, Nakai K and Nakamura H: HitPredict: A database of quality assessed protein-protein interactions in nine species. Nucleic Acids Res 39: D744-D749, 2011.
32. Vasaikar SV, Straub P, Wang J and Zhang B: LinkedOmics: Analyzing multi-omics data within and across 32 cancer types. Nucleic Acids Res 46: D956-D963, 2018.
33. Ye J, Coulouris G, Zaretskaya I, Cutcutache I, Rozen S and Madden TL: Primer-BLAST: A tool to design target-specific primers for polymerase chain reaction. BMC Bioinformatics 13: 134, 2012.
34. Livak KJ and Schmittgen TD: Analysis of relative gene expression data using real-time quantitative PCR and the 2(-Delta Delta C(T)) method. Methods 25:402-408, 2001.
35. Li K, Zhang A, Li X, Zhang H and Zhao L: Advances in clinical immunotherapy for gastric cancer. Biochim Biophys Acta Rev Cancer 1876: 188615, 2021.
36. Zhang C, Liu J, Xu D, Zhang T, Hu W and Feng Z: Gain-of-function mutant p53 in cancer progression and therapy. J Mol Cell Biol 12: 674-687, 2020.
37. Hanahan D: Hallmarks of cancer: New dimensions. Cancer Discov 12: 31-46, 2022.
38. Pitt JM, Marabelle A, Eggermont A, Soria JC, Kroemer G and Zitvogel L: Targeting the tumor microenvironment: Removing obstruction to anticancer immune responses and immunotherapy. Ann Oncol 72: 1482-1492, 2016.
39. Cui Y and Guo G: Immunomodulatory function of the tumor suppressor p53 in host immune response and the tumor microenvironment. Int J Mol Sci 17: 1942, 2016.
40. Qi F, Li J, Qi Z, Zhang J, Zhou B, Yang B, Qin W, Cui W and Xia J: Comprehensive metabolic profiling and genome-wide analysis reveal therapeutic modalities for hepatocellular carcinoma. Research (Wash D C) 6: 0036, 2023.
41. Zetrini AE, Lip H, Abbasi AZ, Alradwan I, Ahmed T, He C, Henderson JT, Ranth AM and Wu X: Remodeling tumor immune microenvironment by using polymer-lipid-manganese dioxide nanoparticles with radiation therapy to boost immune response of castration-resistant prostate cancer. Research (Wash D C) 6: 0247, 2023.
42. Duan X, Du H, Yuan M, Liu L, Liu R and Shi J: Bioinformatics analysis of necroptosis-related lncRNAs and immune infiltration, and prediction of the prognosis of patients with esophageal carcinoma. Exp Ther Med 26: 331, 2023.
43. Chen H, Yu Y, Yang M, Huang H, Ma S, Hu J, Xi Z, Guo H, Yao G, Yang L, et al: YTHDF1 promotes breast cancer progression by facilitating FOXM1 translation in an m6A-dependent manner. Cell Biosci 12: 19, 2022.
44. Pi J, Wang W, Ji M, Wang X, Wei X, Jin J, Liu T, Qiang J, Qi Z, Li F, et al: YTHDF1 Promotes Gastric Carcinogenesis by Controlling Translation of FZD7. Cancer Res 81: 2651-2665, 2021.
45. Chen XY, Liang R, Yi YC, Fan HN, Chen M, Zhang J and Zhu JS: The m6A reader YTHDF1 facilitates the tumorigenesis and metastasis of gastric cancer via USP14 translation in an m6A-dependent manner. Front Cell Dev Biol 9: 647702, 2021.
46. Liu XS, Kui XY, Gao Y, Chen XQ, Zeng J, Liu XY, Zhang Y, Zhang YH and Pei ZJ: Comprehensive analysis of YTHDF1 immune infiltrates and ceRNA in human esophageal carcinoma. Front Genet 13: 835265, 2022.
47. Tsuchiya K, Yoshimura K, Inoue Y, Iwashita Y, Yamada H, Kawase A, Watanabe T, Tanahashi M, Ogawa H, Funai K, et al: YTHDF1 and YTHDF2 are associated with better patient survival and an inflamed tumor-immune microenvironment in non-small-cell lung cancer. OncoImmunology 10: 1962656, 2021.

48. Han D, Liu J, Chen C, Dong L, Liu Y, Chang R, Huang X, Liu Y, Wang J, Dougherty U, *et al*: Anti-tumour immunity controlled through mRNA m^{6}A methylation and YTHDF1 in dendritic cells. Nature 566: 270-274, 2019.

49. Bai X, Wong CC, Pan Y, Chen H, Liu W, Zhai J, Kang W, Shi Y, Yamamoto M, Tsukamoto T, *et al*: Loss of YTHDF1 in gastric tumors restores sensitivity to antitumor immunity by recruiting mature dendritic cells. J Immunother Cancer 10: e003663, 2022.

50. Shevach EM: Fatal attraction: Tumors beckon regulatory T cells. Nat Med 10: 900-901, 2004.

51. Petersen RP, Campa MJ, Sperlazza J, Conlon D, Joshi MB, Harpole DH Jr and Patz EF Jr: Tumor infiltrating Foxp3+ regulatory T-cells are associated with recurrence in pathologic stage I NSCLC patients. Cancer 107: 2866-2872, 2006.

52. Bates GJ, Fox SB, Han C, Leek RD, Garcia JF, Harris AL and Banham AH: Quantification of regulatory T cells enables the identification of high-risk breast cancer patients and those at risk of late relapse. J Clin Oncol 24: 5373-5380, 2006.

53. Gao Q, Qiu SJ, Fan J, Zhou J, Wang XY, Xiao YS, Xu Y, Li YW and Tang ZY: Intratumoral balance of regulatory and cytotoxic T cells is associated with prognosis of hepatocellular carcinoma after resection. J Clin Oncol 25: 2586-2593, 2007.

54. Perrone G, Ruffini PA, Catalano V, Spino C, Santini D, Muretto P, Spoto C, Zingaretti C, Sisti V, Alessandroni P, *et al*: Intratumoural FOXP3-positive regulatory T cells are associated with adverse prognosis in radically resected gastric cancer. Eur J Cancer 44: 1875-1882, 2008.

55. Georgiev P, Charbonnier LM and Chatila TA: Regulatory T cells: The many faces of Foxp3. J Clin Immunol 39: 623-640, 2019.

56. Terranova-Barberio M, Pawlowska N, Dhawan M, Moasser M, Chien AJ, Melisko ME, Rugo H, Rahimi R, Deal T, Daud A, *et al*: Exhausted T cell signature predicts immunotherapy response in ER-positive breast cancer. Nat Commun 11: 3584, 2020.

57. Jin K, Cao Y, Gu Y, Fang H, Fei Y, Wang J, Liu X, Lv K, He X, Lin C, *et al*: Poor clinical outcomes and immunoevasive contexture in CXCL13+CD8+ T cells enriched gastric cancer patients. Oncoimmunology 10: 1915560, 2021.

58. Zarour HM: Reversing T-cell dysfunction and exhaustion in cancer. Clin Cancer Res 22: 1856-1864, 2016.

59. Zhao T, Sun D, Zhao M, Lai Y, Liu Y and Zhang Z: N^6-methyladenosine mediates arsenite-induced human keratinocyte transformation by suppressing p53 activation. Environ Pollut 259: 113908, 2020.

60. Kwok CT, Marshall AD, Rasko JE and Wong JJ: Genetic alterations of m^{6}A regulators predict poorer survival in acute myeloid leukemia. J Hematol Oncol 10: 39, 2017.

61. Xu A, Liu M, Huang MF, Zhang Y, Hu R, Gingold JA, Liu Y, Zhu D, Chien CS, Wang WC, *et al*: Rewired m^{6}A epitranscriptomic networks link mutant p53 to neoplastic transformation. Nat Commun 14: 1694, 2023.

62. Hassin O and Oren M: Drugging p53 in cancer: One protein, many targets. Nat Rev Drug Discov 22: 127-144, 2023.

63. Zeng Y and Jin RU: Molecular pathogenesis, targeted therapies, and future perspectives for gastric cancer. Semin Cancer Biol 86: 566-582, 2022.